# ORTHOGONAL WAVEFORMS FOR LARGE MIMO SONAR SYSTEMS

Yan Pailhas[a] & Yvan Petillot[a]

[a]Ocean Systems Lab, Heriot Watt University

Riccarton Campus, EH14 4AS, Scotland, UK
tel: + 44 (0) 131 451 3357, email: Y.Pailhas@hw.ac.uk, www: http://osl.eps.hw.ac.uk/

***Abstract:*** *MIMO stands for Multiple Inputs Multiple Outputs. Such systems have been developed at first for radar applications. MIMO have recently gained interest in the underwater acoustic community because of certain benefits over traditional systems such as increase resolution or increase in signal to clutter ratio to name a few. The MIMO concept relies on multiple transmitters ($N_t$) sending unique and orthogonal waveforms through the environment. Several receivers ($N_r$) then capture environment, targets or clutter echoes. At each receiver point the total signal is filtered to separate each transmitter signal. The stage at which MIMO systems separate from multi-static systems is at the information processing stage (done centrally rather that separately at each receiver node). Accessing the $N_t \times N_r$ signals requires the orthogonality of the out-coming pulses. As purely orthogonal waveforms do not exist, different approaches were developed to minimise the waveform cross-correlation. Such methods include TDMA (time division multiple access) where waveforms share the same frequency band, but at different times, FDMA (frequency division multiple access) where waveforms occupy different frequencies at the same time, or CDMA (code division multiple access) where waveforms share the same frequencies at the same time. In this paper we review the three main classes of orthogonal waveforms proposed for radar applications. We examine their implications and restrictions for sonar systems. We finally propose a novel CDMA design: the ICMS which suits large MIMO sonar systems and transducer constraints.*

***Keywords:*** *MIMO sonar systems, MIMO waveform design.*

# 1.  MIMO SONAR SYSTEMS

## 1.1.  MIMO sonar formulation

We first present the MIMO formulation for the finite scatterer target model. A target is represented here with $Q$ scattering points spatially distributed. Let $\{X_q\}_{q\in[1,Q]}$ be their locations. The reflectivity of each scattering point is represented by the complex random variable $\zeta_q$. All the $\zeta_q$ are assumed to be zero-mean, independent and identically distributed with a variance of $E[|\zeta_q|^2] = 1/Q$. Let $\Sigma$ be the reflectivity matrix of the target, $\Sigma = \text{diag}(\zeta_1, ..., \zeta_Q)$. By using this notation the average RCS of the target $\{X_q\}$, $E[\text{tr}(\Sigma\Sigma^H)]$, is normalised to 1.

The MIMO system comprises a set of $K$ transmitters and $L$ receivers. Each transmitter $k$ sends a pulse $\sqrt{E/K}.s_k(t)$. We assume that all the pulses $s_k(t)$ are normalised. Then $E$ represents the total transmit energy of the MIMO system. Receiver $l$ receives from transmitter $k$ the signal $z_{lk}(t)$ which can be written as:

$$z_{lk}(t) = \sqrt{\frac{E}{K}} \sum_{q=1}^{Q} h_{lk}^{(q)} s_k\left(t - \tau_{tk}(X_q) - \tau_{rl}(X_q)\right) \tag{1}$$

with $h_{lk}^{(q)} = \zeta_q \exp\left(-j2\pi f_c[\tau_{tk}(X_q) + \tau_{rl}(X_q)]\right)$. $f_c$ is carrier frequency, $\tau_{tk}(X_q)$ represents the propagation time delay between the transmitter $k$ and the scattering point $X_q$, $\tau_{rl}(X_q)$ represents the propagation time delay between the scattering point $X_q$ and the receiver $l$. Note that $h_{lk}^{(q)}$ represents the total phase shift due to the propagation and the reflection on the scattering point $X_q$. Assuming the $Q$ scattering points are close together (*i.e.* within a resolution cell), we write:

$$s_k\left(t - \tau_{tk}(X_q) - \tau_{rl}(X_q)\right) \approx s_k\left(t - \tau_{tk}(X_0) - \tau_{rl}(X_0)\right) = s_k^l(t, X_0) \tag{2}$$

where $X_0$ is the centre of gravity of the target $\{X_q\}$. So Eq. (1) can be rewritten as:

$$z_{lk}(t) = \sqrt{\frac{E}{K}} s_k^l(t, X_0) \times \left(\sum_{q=1}^{Q} \zeta_q \exp\left(-j2\pi f_c[\tau_{tk}(X_q) + \tau_{rl}(X_q)]\right)\right) = \sqrt{\frac{E}{K}} \left(\sum_{q=1}^{Q} h_{lk}^{(q)}\right) s_k^l(t, X_0) \tag{3}$$

## 1.2.  ATR capabilities

In this section we are interested in the MIMO intensity response of an object: $\sum_{q=1}^{Q} h_{lk}^{(q)}$ from Eq. (3). Lets assume that the reflectivity coefficients $\zeta_q$ can be modelled by the random variable $\frac{1}{\sqrt{Q}} e^{2i\pi U}$ where $U \in [0,1]$ is the uniform distribution. The central limit theorem then gives us the asymptotic behaviour of the target intensity response, and we can write:

$$\lim_{Q \to +\infty} \sqrt{\left|\sum_{q=1}^{Q} h_{lk}^{(q)}\right|^2} = \text{Rayleigh}(1/\sqrt{2}) \tag{4}$$

The convergence of Eq. (4) is fast. However for a small number of scatterers (typically $Q \le 5$), the target reflectivity PDF exhibits noticeable variation from the Rayleigh distribution.

Assuming that man-made targets can be effectively modelled by a small number of scatterers, we can take advantage of the dissimilarities of the reflectivity PDF functions to estimate the number of scattering points. Each observation is a realisation of the random variable $\gamma_n = \sqrt{\left|\Sigma_{q=1}^{Q} h_{lk}^{(q)}\right|^2}$ with $Q$ the number of scattering points. Each set of observations $\Gamma = \{\gamma_n\}_{n \in [1,N]}$ where $N$ is the number of views represents the MIMO output. Given $\Gamma$, we can compute the probability that the target has $Q$ scatterers using Bayes rules:

$$P(T_Q|\Gamma) = \frac{P(\Gamma|T_Q)P(T_Q)}{P(\Gamma)} \tag{5}$$

where $T_Q$ represents the event that the target has $Q$ scatterers. Assuming independent observations, 4 target types and no *a priori* information about the target we have:

$$P(T_Q|\Gamma) = \frac{\prod_{n=1}^{N} P(\gamma_n|T_Q)}{\sum_{Q=2}^{5+} P(\Gamma|T_Q)} \tag{6}$$

The estimated target class corresponds to the class which maximises the conditional probability given by Eq. (6). Figure 1 draws the probability of correct classification for each class depending on the number of views based on $10^6$ classification experiments. With only 100 views, the overall probability of correct classification is great than 92%.
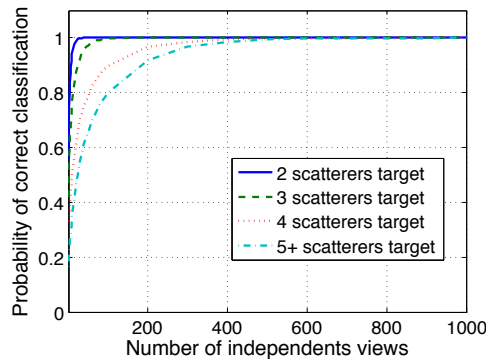


*Fig. 1: Correct classification probability against the number of independent views for 4 classes of targets (2, 3, 4 and 5+ scattering points targets).*

### 1.3. Super-resolution capabilities

Let $r_l(t)$ be the total received signal at the receiver $l$. We can write $r_l(t) = \sum_{k=1}^{K} z_{lk}(t)$. The target response $x_{lk}$ from the MIMO system is then the output of the filter bank $s_k^*(t)$ with $k \in [1,K]$. With our notations and assuming orthogonal waveforms, we arrive to:

$$x_{lk} = r_l \star s_k^*(t) = \sum_{q=1}^{Q} h_{lk}^{(q)} \tag{7}$$

The average target echo intensity from all the bistatic views is given by:

$$\mathcal{F}(\mathbf{r}) = \frac{1}{N} \sum_{l,k} ||x_{lk}||^2 \tag{8}$$

Using the same target probability distribution stated in the model presented earlier (cf. section 1.1), we deduce that $\mathcal{F}(\mathbf{r})$ follows the probability distribution:

$$\mathcal{F}(\mathbf{r}) \sim \frac{1}{N} \sum_{n=1}^{N} \text{Rayleigh}^2(\sigma) \sim N.\Gamma(N, 2\sigma^2) \tag{9}$$

where $\Gamma$ is the Gamma distribution. Note that the second equivalence is given using the properties of the Rayleigh distribution. The asymptotic behaviour of $\mathcal{F}(\mathbf{r})$ can be deduced from the following identity [1]:

$$\lim_{N \to +\infty} N.\Gamma(Nx, N, 1) = \delta(1 - x) \tag{10}$$

Eq. 10 shows that the MIMO mean target intensity $\mathcal{F}(\mathbf{r})$ converges toward the RCS defined in section 1.1 which means that the scatterers within one resolution cell decorrelate between each other. MIMO systems then solve the speckle noise in the target response. This demonstrates why super-resolution can be achieved with large MIMO systems.


## 2. WAVEFORM DESIGN FOR MIMO RADAR

### 2.1. TDMA: Time Division Multiple Access

TDMA refers to Time Division Multiple Access. It refers to waveform sets sharing the same frequency band but not int the same time. Pulses are transmitted successively at regular interval $\Delta_\tau$ called the pulse repetition interval (PRI). This strategy is by far the most commonly used for multi-static sonar systems. And as long as $\Delta_\tau$ is large enough for the sound to fall below the detection threshold, the TDMA waveforms are quasi-orthogonal. The intrinsic problem with TDMA is related to the dynamic of the scene. In an ASW (anti-submarine warfare) context for example, one may require to survey a large area. If the maximum distance is 40km, taking into account the relatively slow sound speed in water, the PRI can be as high as 1 minute. A 15 knots target would then potentially move $\frac{1}{2}$km between pings. The tracking related to such system would then be diminished by the data association stage due to the rapidly growing position uncertainty.


### 2.2. FDMA: Frequency Division Multiple Access

FDMA refers to Frequency Division Multiple Access. In this case the waveform set occupy different frequency band at the same time. As long as the frequency bands of each waveform are well separated, the waveforms are almost orthogonal. Different strategies have been explored to implement FDMA depending on the slicing of the available frequency band. Each pulse can occupy for example a different continuous frequency band or having finely interleaved frequency supports. For active sonar however, the bandwidth is a rare resource. Assuming identical transmitters, a FDMA approach results in dividing the full bandwidth by the number of transmitters and then potentially losing all benefit of wideband systems including SNR and resolution loss.

### 2.3. CDMA: Code Division Multiple Access

Due to the restrictions of the two previous approach in orthogonal waveforms, a lot of effort has been put in code division multiple access (CDMA) approaches. CDMA waveforms include polyphase code, pseudorandom phase codes, up and down chirps or codes such as Baker or Gold codes. The main criteria for MIMO waveform are the sidelobe level and cross correlation. Several optimisation solutions were proposed using SA (Simulated Annealing) algorithms [2, 3], Bee algorithms [4] or maximal length sequences [5]. In [6], Rabideau introduces another metric to measure the fitness of MIMO waveforms by considering the maximum amount of interference that can be cancelled. He then applied his metric for clutter reduction adaptive MIMO system. Another approach to CDMA waveform design is to relax the orthogonality hypothesis and optimising the waveform covariance matrix according to a certain criteria. Forsythe in [7] for example computed the covariance matrix which maximises the image intensity. Li then proposed in [8] a cyclic algorithm to compute the covariance matrix under the constant amplitude constraint. In [9], Yang derives optimum waveform design to maximise MI (Mutual Information) and minimising mean-square error (MMSE) for target response estimation.
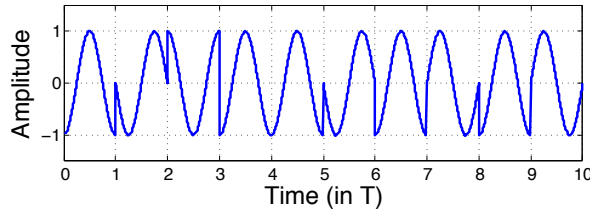


*Fig. 2: Example of phased coded radar waveform.*

## 3. ORTHOGONAL WAVEFORMS FOR MIMO SONAR

Radar design and electronics impose a certain number of constraints on the waveform design. One of the most restrictive is due to the non-linear amplifiers used for such systems and imposes to the radar waveform a constant amplitude. Although the constant amplitude requirement maximises the pulse energy, it drastically reduces the degrees of freedom. The radar community then find efficient solutions to manipulate the signal phase including phase shift. Figure 2 provides an example of phased coded radar used in [5]. For active sonar system, pulse emission is the result of piezo-electric material excitation via linear amplifiers. Sonar systems are then not constraint to pulses with constant amplitude. The transducers however cannot handle drastic phase shift and phased coded waveforms may be extremely distorted through PZT transducers.

In this paper we are interested in the orthogonal waveform families. Section 1 highlighted the importance of both orthogonality and independence of the MIMO signals for recognition tasks and/or for imagery purposes. Orthogonality is indeed needed in Eq. (5) to derive the target intensity function for each MIMO pair and in Eq. (7) to recover the target signal from each Tx/Rx path. All derived results including MIMO autofocus algorithms [10] then depends on the waveform orthogonality. So far only TDMA or FDMA waveforms have been tested for orthogonal waveform design. The only exception is the CDMA waveforms known as up and

down chirps. The up and down chirp strategy however only provides two pseudo-orthogonal pulses and it is then inadequate for large MIMO systems. In this section we propose a CDMA strategy which fits the requirements of wideband large MIMO sonar systems:

1. wideband width covered by every pulses

2. *'good'* auto- and cross-correlation functions

3. possibility to generate a large number of orthogonal waveforms

4. waveforms with smooth phase transition

5. waveforms with relative constant amplitude

Note that if sonar amplifier electronics relax the strict constant amplitude constraint, a relative constant amplitude helps to maintain a high energy pulse and then maximise the signal to noise ratio. To fulfil the requirements previously stated, we propose to build the MIMO sonar waveforms using interlaced micro-chirp series (IMCS) with constant bandwidth. The waveform is the summation of two concatenations of micro-chirps series with equal duration $\tau$. The second micro-chirps series is time shifted relative to the first one by a factor of $\frac{\tau}{2}$. Figure 3(a) draws the envelops of interlaced two micro-chirp series.



(a)                                      (b)
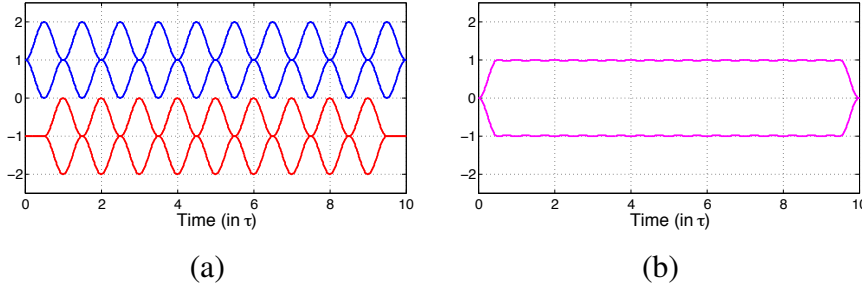
*Fig. 3:* (a) *envelop of the concatenated micro-chirps (blue curve) and the interlaced concatenated micro-chirps (red curve).* (b) *full IMCS waveform envelop.*

Each micro-chirp has the same duration $\tau$ and the same windowing. In this paper we chose the Hanning tapering function. The windowing function function is threefold:

- it smoothes the phase transition between each consecutive micro-chirp

- it ensures a relatively constant amplitude for the overall waveform (as shown in Fig. 3(b))

- it constrains the micro-chirp to a constant bandwidth

The full available bandwidth $B$ is divided into $N_B$ equal sub-bandwidth. The size of the minimal sub-bandwidth is given by the micro-pulse duration $\tau$ and the windowing function and can be approximated in our case by $1/\tau$. $N_B$ can then approximated by $B.\tau$.
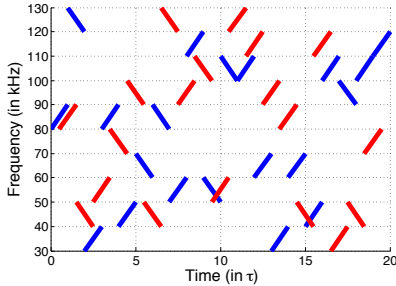
*Fig. 4: Example of an IMCS waveform structure in the time-frequency domain. The blue segments represent the micro-chirps of the first series, the red ones represent the second series.*

The duration of the full waveform is $\tau.N_\tau$ where $N_\tau$ is the number of micro-chirps of the first $\mu$-chirp series. Each $\mu$-chirp is chosen randomly between the $N_B$ sub-bands with a random up or down chirp structure. The randomised up or down structure minimised the cross-correlation as well as the sidelobes in the auto-correlation function. Figure 4 draws an example of IMCS waveform structure in the time-frequency plane. Blue and red segments represent respectively the $\mu$-chirp structure of the first and second $\mu$-chirp series.

Theoretically there are $(2N_B)^{2N_\tau-1}$ different waveforms. We computed 100 different waveforms for $B = [30$ kHz $- 130$ kHz$]$, $\tau = 10^{-4}$s, $N_B = 10$ and $N_\tau = 90$. Figure 5(a) displays the waveform covariance matrix. For perfectly orthogonal waveforms, we expect the covariance matrix being the identity matrix $I_N$. Figure 5(b) shows the auto-correlation function and very low cross-correlation function of one particular waveform.



(a)



(b)
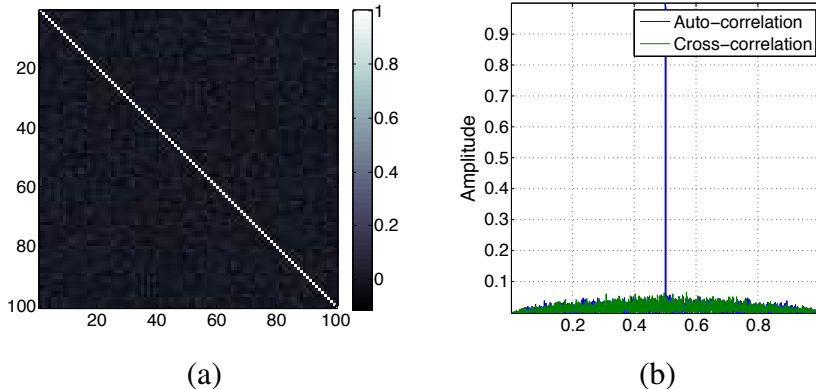
*Fig. 5:* (a) *Waveform covariance matrix.* (b) *Example of auto-correlation (blue curve) and cross-correlation (green curve) functions of the proposed waveforms.*

## 4. CONCLUSION

In paper we explore the diverse strategies for orthogonal waveforms proposed for MIMO radar applications. Because most of the strategies are based on phase coded signals, they proved to be inadequate for sonar transducers. We proposed a novel CDMA waveform: the IMCS which fits the requirement for large wideband MIMO sonar systems. The IMCS combines the coverage of the full frequency band for each waveform, very low cross-correlation functions

and minimal sidelobes for the auto-correlation functions. The signal phase varies slowly and is suitable for piezo-electric transducers. Future work includes the testing of the IMCS waveforms in real environments to assess their robustness against noise, clutter or multi-path.

## 5. ACKNOWLEDGEMENT

## REFERENCES

[1] Y. Pailhas. *Sonar Systems for Objects Recognition*. PhD thesis, Heriot-Watt University, 2012.

[2] Hai Deng. Polyphase code design for orthogonal netted radar systems. *Signal Processing, IEEE Transactions on*, 52(11):3126–3135, Nov 2004.

[3] A. Aubry, M. Lops, A.M. Tulino, and L. Venturino. On mimo waveform design for non-gaussian target detection. In *Radar Conference - Surveillance for a Safer World, 2009. RADAR. International*, pages 1–6, Oct 2009.

[4] Milad Malekzadeh, Alireza Khosravi, Saeed Alighale, and Hamed Azami. Optimization of orthogonal poly phase coding waveform based on bees algorithm and artificial bee colony for mimo radar. In De-Shuang Huang, Changjun Jiang, Vitoantonio Bevilacqua, and JuanCarlos Figueroa, editors, *Intelligent Computing Technology*, volume 7389 of *Lecture Notes in Computer Science*, pages 95–102. Springer Berlin Heidelberg, 2012.

[5] M. Harika Rao, G. V. K. Sharma, and K. Raja Rajeswari. Orthogonal phase coded waveforms for mimo radars. *International Journal of Computer Applications*, 63(6):31–35, February 2013.

[6] Daniel J. Rabideau. Adaptive mimo radar waveforms. In *Radar Conference, 2008. RADAR '08. IEEE*, pages 1–6, May 2008.

[7] K.W. Forsythe and D.W. Bliss. Waveform correlation and optimization issues for mimo radar. In *Signals, Systems and Computers, 2005. Conference Record of the Thirty-Ninth Asilomar Conference on*, pages 1306–1310, October 2005.

[8] Jian Li, Petre Stoica, and Xumin Zhu. Mimo radar waveform synthesis. In *Radar Conference, 2008. RADAR '08. IEEE*, pages 1–6, May 2008.

[9] Yang Yang and R.S. Blum. Mimo radar waveform design based on mutual information and minimum mean-square error estimation. *Aerospace and Electronic Systems, IEEE Transactions on*, 43(1):330–343, January 2007.

[10] Yan Pailhas and Yvan Petillot. Synthetic aperture imaging and autofocus with coherent mimo sonar systems. In *Synthetic aperture sonar & synthetic aperture radar conference*, 2014.